HHS Public Access

Author manuscript

Dev Neurobiol. Author manuscript; available in PMC 2020 September 09.

Published in final edited form as:

Dev Neurobiol. 2016 September ; 76(9): 956–971. doi:10.1002/dneu.22368.

FGF Signaling Enhances a Sonic Hedgehog Negative Feedback Loop at the Initiation of Spinal Cord Ventral Patterning

Aixa V. Morales[#1], **Sergio Espeso-Gil**[1,*], **Inmaculada Ocaña**[1,2], **Francisco Nieto-Lopez**[1,2,3], **Elena Calleja**[1], **Paola Bovolenta**[1,2,3], **Mark Lewandoski**[4], **Ruth Diez del Corral**[#1,†]

[1]Instituto Cajal, Consejo Superior de Investigaciones Científicas, Madrid 28002, Spain

[2]CIBER de Enfermedades Raras, Spain

[3]Centro de Biología Molecular "Severo Ochoa," Consejo Superior de Investigaciones Científicas-UAM, Cantoblanco 28049, Spain

[4]Cancer and Developmental Biology Laboratory, Center for Cancer Research, National Cancer Institute, Frederick, Maryland 21702, USA

[#] These authors contributed equally to this work.

Abstract

A prevalent developmental mechanism for the assignment of cell identities is the production of spatiotemporal concentration gradients of extracellular signaling molecules that are interpreted by the responding cells. One of such signaling systems is the Shh gradient that controls neuronal subtype identity in the ventral spinal cord. Using loss and gain of function approaches in chick and mouse embryos, we show here that the fibroblast growth factor (FGF) signaling pathway is required to restrict the domains of ventral gene expression as neuroepithelial cells become exposed to Shh during caudal extension of the embryo. FGF signaling activates the expression of the Shh receptor and negative pathway regulator *Patched 2 (Ptch2*) and therefore can enhance a negative feedback loop that restrains the activity of the pathway. Thus, we identify one of the mechanisms by which FGF signaling acts as a modulator of the onset of Shh signaling activity in the context of coordination of ventral patterning and caudal axis extension.

Keywords

chick embryo; mouse embryo; neural tube; gene regulatory network; FGF; Shh; Ptch

INTRODUCTION

Development of the nervous system involves the control of proliferation, cell cycle exit and cell fate assignment which depend on the position of neural progenitors and neurons at their birth time. The spinal cord of amniotes derives from a caudal primordium located in the

Correspondence to: R. Diez del Corral (r.diez@cajal.csic.es) or A.V. Morales (aixamorales@cajal.csic.es).
[*]Present address: Centro de Regulación Genómica, Barcelona, 08003, Spain
[†]Present address: Champalimaud Neuroscience Program Champalimaud Center for the Unknown, 1400-038, Lisbon, Portugal

Additional Supporting Information may be found in the online version of this article.

vicinity of the node, which regresses with the primitive streak, progressively leaving in its wake spinal cord cells (Brown and Storey, 2000; Mathis et al., 2001). Although the signaling pathways important for cell fate assignment along the dorso-ventral axis and for caudal extension of the spinal cord are known, their interactions and temporal control have not been fully elucidated yet.

Ventral patterning genes encode transcription factors (i.e. FoxA2, Nkx2.2, Nkx6.1, and Olig2) that, in combination, allow the specification of motor neurons and different types of interneurons in a spatially and temporally ordered way (Briscoe et al., 2000). The restricted expression pattern of these genes along the dorso-ventral axis depends on Sonic Hedgehog (Shh) signaling that is activated in a ventral to dorsal gradient in spinal cord progenitor cells exposed to Shh, emanating from the notochord and the floor plate (Jessell, 2000). The core Shh signaling pathway involves the receptors Patched 1 and Patched 2 (Ptch1, Ptch2) which, in the absence of Shh, block the activity of the transmembrane protein Smoothened (Smo). With Smo active, an intracellular cascade leads to the accumulation of activator forms of Gli transcription factors and the reduction of Gli repressive forms that, in turn, act on appropriate target genes (Dessaud et al., 2008).

The strict control of Shh concentration, timing of exposure and response is achieved, in part, by several positive and negative feedback loops, as well as by modulators of the pathway (Dessaud et al., 2008; Ribes and Briscoe, 2009). One important negative feedback loop results from the ability of Shh to activate transcription of *Ptch1* and *Ptch2* which, in turn, can limit Smo function and Shh spreading across the tissue (Goodrich et al., 1996, 1997; Marigo and Tabin, 1996; Pearse et al., 2001; Jeong and McMahon, 2005; Vokes et al., 2007; Holtz et al., 2013; Alfaro et al., 2014). Thus, for instance, overexpression of *Ptch1* or *Ptch2* in the chick spinal cord downregulates expression of Nkx6.1, which is one of the factors induced by Shh (Holtz et al., 2013).

Neural progenitors become exposed to Shh from the notochord when they leave the spinal cord primordium region. However, the expression of ventral specification transcription factors that require Shh signaling only starts as cells progress into the neural tube flanked by somites (Diez del Corral et al., 2003; Novitch et al., 2003). This delay has been related to changes in FGF signaling (Diez del Corral et al., 2003; Novitch et al., 2003), which is specifically required for the maintenance of cells within the spinal cord primordium (Mathis et al., 2001). Downregulation of FGF signaling is critical for the transition from an immature spinal cord primordium to a more mature spinal cord state where neuronal differentiation (Diez del Corral et al., 2002), neural crest cell specification and emigration (Martinez-Morales et al., 2011) and expression of a number of ventral patterning genes can occur (Bertrand et al., 2000; Diez del Corral et al., 2003; Novitch et al., 2003).

Here, we demonstrate that FGF signaling is required for the proper dorso-ventral restriction of progenitor domains and for the expression of the Shh receptor and pathway inhibitor *Ptch2*. This regulation of a negative feedback loop at the core of the Shh pathway by FGF signaling would modulate the onset of Shh signaling in the ventral spinal cord.

MATERIALS AND METHODS

DNA Constructs

PCIGs (*pCAGGS-IRES*–nuclear *EGFP* (Megason and McMahon, 2002) or *pCAGGS-IRES–EGFP*) were used as expression vectors, unless stated otherwise, and were the control DNA in electroporation experiments. *DN-FGFR* encodes a truncated chick FGFR1c (aa 1–425) provided by C. Weijer (University of Dundee, Dundee, Scotland, UK; Yang et al., 2002). Mouse *Etv4* was obtained from C. Tabin (Brent and Tabin, 2004). Human *GliA* encodes a truncated version of Gli3 (amino acids 468–1580 of hGli3) that behaves as a constitutively activator form of Gli targets (Stamataki et al., 2005). Mouse *FGF8b* was obtained from T. Schimmang (Dominguez-Frutos et al., 2009).

Mouse *Ptch2* was obtained by PCR amplification of mouse cDNA and ligated in frame to *Cherry* at its 5′ end and the HA-epitope at its 3′ end and inserted in the *PCAGGS* expression vector. For the luciferase reporter construct, a fragment from genomic chick *Ptch2* was obtained by PCR amplification with primers (FWD: TTTAAGCTTTCTCGGTCGGTTG TGG and REV: TTTGTGACAGGGATGGCTGCGGA CA) and cloned in PGL3-promoter.

In Ovo Electroporation

Chick embryos were electroporated with purified plasmid DNA (1–2 μg/μL) as previously described (Martinez-Morales et al., 2011) and they were analysed 24 h postelectroporation.

Explant Cultures and Pharmacological Treatments

Explants were dissected from HH9–13 chicken embryos. Three different types of explants including the region of the neural plate or tube adjacent to presomitic mesoderm were isolated (as depicted in Fig. 4): (1) pNT explants correspond to neural tissue caudal to the last formed somite and rostral to the node [Figs. 2(A) and 4(K), and Supporting information Fig. (2)], (2) one side pNT without floor plate is a similar explant containing only one hemitube and devoid of the floor plate region [Fig. 4(F)], and (3) pNT explants with mesoderm, endoderm and node extend more caudally to include the node and adjacent tissue [Fig. 4(A)]. For neural only explants, mesoderm was removed with trypsin treatment (Diez del Corral et al., 2002). Explants were cultured in collagen beds as previously described (Martinez-Morales et al., 2011) in medium containing either BSA only, 330 to 660 ng/mL of human FGF4 (Sigma) or mouse FGF8b (Sigma) (both supplemented with 1–10 ng/μL heparin) or containing 10 μM PD184352 (Axon Medchem), 10 μM PD173074 (Sigma), 1 to 10 μM SANT1 (Calbiochem), 0.1% DMSO, or combinations of the different compounds as indicated.

Down-regulation of the FGF signaling target *Sprouty2* in node region explants (Minowada et al., 1999) and of *Pax6* in neural explants (Diez del Corral et al., 2003) were monitored to confirm down-regulation or activation of FGF signaling, respectively.

Mouse Mutants

Female mice homozygous for a floxed allele of *Fgfr1* (Xu et al., 2002) were crossed to males homozygous for TCre (Perantoni et al., 2005) and heterozygous for the *Fgfr1* null allele (the Cre- mediated derivative of the floxed allele). The progeny of this cross are 50% mutant (TCre; $Fgfr1^{flox/null}$) and 50% control (T-Cre; $Fgfr1^{flox/+}$). The first few litters were identified by PCR-genotyping, and after that via phenotyping as the abnormal caudal extension defect was obvious (Wahl et al., 2007).

In Situ Hybridization

Embryos were fixed overnight at 4°C and *in situ* hybridisation with digoxigenin labelled probes was performed following standard methods. Embryos were embedded in 5% agarose/10% sucrose and sectioned on a vibratome (40 μm; VT1000S; Leica). Chick *Smo* probe was synthesized from EST clone pgn1c.pk009.m19 (Carre et al., 2006) (University of Delaware collection) and mouse *Ptch2* probe corresponds to a 2440 bp fragment (nucleotide 1110 to 3549 of NM_008958) which is longer than the probe previously described in Motoyama et al. (1998) and Takabatake et al. (1997) corresponding to a 766 bp cDNA fragment (AB000847). Other probes used have been described in the literature: chick *FoxA2, Gli1, Gli2, Gli3, Ptch1, Ptch2, Shh*, and *Spry2*.

Immunohistochemistry

Embryos were fixed for 2 to 4 h at 4°C with 4% PFA in PBS, and they were immersed in 30% sucrose solution, embedded in 7.5% gelatin/15% sucrose and sectioned on a cryostat (15 μm; CM1900; Leica). For immunohistochemistry, 15 μm cryostat were permeabilised with 0.5% Triton X-100, blocked with 10% FBS, and incubated overnight at 4°C with the primary antibody. After washing, the cryostat sections were incubated for 1 h with secondary antibodies. Polyclonal primary antibodies against Olig2 (Millipore: AB9610) were used. Monoclonal antibodies against FoxA2 (4C7), Nkx2.2 (74.5A5), Nkx6.1 (F55A10), and Shh (5E1) were all obtained from the Developmental Studies Hybridoma Bank (developed under the auspices of the National Institute of Child Health and Development and maintained by the University of Iowa). Alexa Fluor 488, Alexa Fluor 647, and Cy3-conjugated antimouse or rabbit secondary antibodies (Invitrogen and Jackson Immunoresearch) were used for detection and nuclei were stained with bisbenzimide. Sections were mounted in Mowiol and photographed using a confocal scanner microscope (SP5; Leica). Cell counting was carried out in four to eight sections of three to six different embryos from each experimental condition.

Analysis of Mouse Mutant Embryos

In order to identify alterations in the onset of ventral patterning we analyzed transverse sections of the caudal regions of mouse embryos. As somites in the *TCre;* $Fgfr1^{flox/null}$ embryos were not correctly formed or were misshaped (Wahl et al., 2007), we could not use them as a reference of the rostrocaudal level and thus, focused our attention on the notochord. The caudal-most notochord appears as a dispersed group of cells, that aggregate in a large bulge and then becomes rod-shaped at more rostral presomitic regions. For each embryo we performed double immunohistochemistry and identified the most caudal sections

that included the rod-shaped notochord, cells expressing Nkx6.1 or cells expressing Olig2. This allowed us to determine the number of sections and therefore the distance that separated them (each section is 15 μm thick). Data correspond to mean±SEM.

Luciferase Reporter Assay

Transcriptional activity assays were performed in embryos electroporated with the indicated expression DNA constructs, together with the luciferase reporter to be tested and two *Renilla* luciferase constructs carrying either the cytomegalovirus or the simian virus 40 promoter (Promega, Southampton, UK) for normalization. Luciferase activities were measured by the Dual Luciferase Reporter Assay System (Promega). Both sides of the tube were electroporated by changing the electrode polarity. Eggs were further incubated for 6 h and were assayed for EGFP expression in the neural tube and the electroporated region was dissected (only levels adjacent to paraxial mesoderm and last four somites where considered), frozen and processed for luciferase assays. Experiments were performed two times with four individual samples per treatment and measures were normalized to the same day mean value of control samples. Data were analysed using IBM SSPS software to perform one-way ANOVA followed by the Tamhane *post hoc* test for pairwise comparison when variances are not equal. Data correspond to mean±SEM.

Sequence Analysis, Comparison, and Motif Identification

Available chick genomic sequences at public databases (UCSC genome browser galGal4 assembly) present gaps at the predicted 5′ end and intron 2 of the *Ptch2* gene. We have PCR amplified and sequenced genomic DNA corresponding to the gaps using primers from the flanking regions (Genebank accession numbers: KJ433682 and KJ433683) to reconstitute the complete *Ptch2* genomic DNA sequence.

Genomic regions of *Ptch2* from different species were compared with the ERC browser (http://ecrbrowser.dcode.org/) to identify conserved regions that were subsequently analysed to identify possible Gli and ETS binding sites. For GBS, we searched for the sequence TGGGTGGTC with one mismatch allowed, (Kinzler and Vogelstein, 1990; Hallikas et al., 2006; Vokes et al., 2007) and for ETS consensus we searched for GGA(A/T) (Wei et al., 2010).

RESULTS

FGF Signaling is Required for Correct Ventral Patterning

In order to determine whether FGF signaling is required for correct ventral patterning of the neural tube, we electroporated a dominant-negative form of the FGF receptor 1 (*DN-FGFR1-pCIG*) (Martinez-Morales et al., 2011) in the caudal presomitic neural tube (pNT) of Hamburger and Hamilton (HH) stages 11-13 chick embryos and analysed the expression of ventral neural identity markers (Briscoe et al., 2000; Novitch et al., 2001; Ribes et al., 2010) after 20 h.

Blockade of FGF signaling caused a broadening and dorsal shifting of the domains of the motor neuron and ventral interneuron type 3 progenitors, identified by Olig2 and Nkx2.2,

respectively, when compared with the non-electroporated hemitube [Fig. 1(D,G)]. The Nkx6.1 expression domain (from progenitors of ventral interneuron type 2 to floor plate) was only slightly increased [$n = 4/6$; Fig. 1(E)] and no clear change in the extent of the FoxA2 expressing domain (floor plate) was observed in comparison with the non electroporated side ($n = 5/6$; Supporting information Fig. 1). By contrast, no side to side differences were observed in embryos electroporated with the control expression vector (*pCIG*) for any of the markers [Fig. 1(A,B,G)].

As Nkx.2.2, Nkx6.1, and Olig2 expression depends on the Shh signal (Briscoe et al., 2000; Cai et al., 2000; Lu et al., 2000), changes in their expression domains could be due to an increase in Shh expression. However, there were no apparent changes in Shh levels following electroporation of *DN-FGFR1* [$n = 4/4$; Fig. 1(F)] compared with control *pCIG* electroporated embryos [$n = 4/4$; Fig. 1(C)] by immunostaining and also by Western blot analysis of the dissected neural tube (without notochord) after both-side-electroporation (see Supporting Information Materials and Methods and Supporting Information Fig. 2). These data indicate that a decrease in FGF signaling can alter the ventral pattern, without changing noticeably the amount of Shh produced by floor plate cells.

FGF Promotes Transient Induction of the Shh Signaling Modulator *Ptch2*

The effect of FGF on ventral patterning was further examined in pNT explants [Fig. 2(A)]. Exposure to FGF4 for 8 h has been shown to impair the expression of ventral patterning genes such as *Nkx6.1* (Diez del Corral et al., 2003) and we extended this analysis to examine *FoxA2*, another neural target of the pathway, and generic readouts such as *Gli1* (Marigo and Tabin, 1996) and *Ptch1* (Lee et al., 1997; Vokes et al., 2007). A clear down-regulation of *FoxA2* ($n = 8$; Fig. 2(C)] and both *Gli1* [$n = 11$; Fig. 2(E)] and *Ptch1* [$n = 7$; Fig. 2(G)] expression was observed in the presence of FGF4 in comparison with BSA treated explants [$n = 7$, 11, and 8, respectively; Fig. 2(B,D,F)], consistent with a decrease in Shh signaling pathway activity in the presence of FGF. These results indicate that the Shh pathway is susceptible of attenuation by FGF in the presomitic neural tube, a region in which key components of the pathway (Smo, Ptch1 and Ptch2, and Gli1-3) are present [Supporting Information Fig. 3(A-G)] (Marigo and Tabin, 1996; Quirk et al., 1997; Pearse et al., 2001; Diez del Corral et al., 2003; Novitch et al., 2003).

To determine possible immediate changes in the expression of core Shh components, we analysed pNT explants exposed to FGF4 for 2 or 4 h (Fig. 2 and Supporting Information Fig. 4). Short-term exposure (2 h and 4 h) did not affect *Shh* expression [$n = 4$ for each time period; Fig. 2(I); Supporting Information Fig. 4(C)] in comparison with BSA treated explants [$n = 4$ for each time period; Fig. 2(H) and Supporting Information Fig. 4(B)]. By contrast, a similar treatment reduced *Gli1* [$n \geq 4$ for each time period; Fig. 2(K) and Supporting Information Fig. 4(E)] and more dramatically *Ptch1* levels [$n \geq 4$; Fig. 2(M) and Supporting Information Fig. 4(G)] with respect to BSA treated explants [($n \geq 4$ for each time period; Fig. 2(J, L) and Supporting information Fig. 4(D,F)]. However, the observed *Ptch1* and *Gli1* reductions in chicken explants are more likely consequences and not causes of the Shh pathway attenuation (Marigo and Tabin, 1996; Lee et al., 1997; Vokes et al., 2007) as *Gli1* mutant embryos do not exhibit ventral patterning defects (Park et al., 2000) and the

Ptch1 mutation is associated with an expansion and not a reduction of ventral gene expression (Goodrich et al., 1997).

The expression of the other Shh receptor *Ptch2* [highly present in the caudal pNT; Supporting information Fig. 3(D)] displayed instead the most interesting response. It has been previously shown that *Ptch2* expression is down-regulated in explants after 8 h culture in the presence of FGF4 (Diez del Corral et al., 2003) and we have also confirmed this down-regulation after 8 h treatment with FGF8 ($n = 10$; Fig. 2(N,O)]). However, *Ptch2* was strongly upregulated after 2 h and 4 h in the presence of either FGF4 or FGF8 [$n \geq 7$ for each time period and treatment; Fig. 2(P,Q), Supporting Information Fig. 4(H-K)]. Moreover, this up-regulation was dependent on the FGFR-MAPK pathway as *Ptch2* levels did not increase in explants treated with FGF in the presence of either the FGFR antagonist PD173074 or the MAPK kinases MEK1 and MEK5 antagonist PD184352 (Mohammadi et al., 1998; Sebolt-Leopold et al., 1999) [$n = 3$ to 4 for each treatment, Fig. 2(R-U)]. These results indicate that *Ptch2* is an early transcriptional response target of FGF signaling which may be responsible for the FGF mediated repression of the Shh pathway and ventral patterning genes.

Overexpression of *Ptch2* in the chick spinal cord has been shown to affect the expression of Shh responsive genes, down-regulating Nkx6.1 and upregulating Pax7 (Holtz et al., 2013). We have electroporated mouse *Ptch2* in the chick spinal cord and confirm a clear reduction of Nkx6.1 [$n = 5/5$; Fig. 3(A-A′)] and show a reduction of the more ventral progenitor domains identified by Nkx2.2 [$n = 3/3$; Fig. 3(B-B′)] and Olig2 [$n = 4/5$; Fig. 3(C-C')], as expected for a Shh pathway inhibitor.

These results reveal the Shh pathway modulator Ptch2 as a possible mediator of FGF function in the control of neural tube ventral patterning.

FGF and Shh are Cooperatively Required to Activate *Ptch2*

To examine whether FGFR-MAPK signaling can not only promote *Ptch2* expression but it is also necessary for its expression, explants containing the node and the surrounding neural plate, mesoderm and endoderm [Fig. 4(A)] were treated with the MAPK kinase antagonist PD184352. In this condition, *Ptch2* expression was severely downregulated after 4 h in comparison with DMSO treated explants [$n \geq 12$ for each treatment; Fig. 4(B,C)], supporting an important role for the FGF-MAPK pathway on the onset of *Ptch2* expression.

Expression of *Ptch2* in the midline of early embryos depends on Shh signaling (Pearse et al., 2001). Interestingly, *Ptch2* expression in caudal tissue explants [Fig. 4(A)] was down-regulated in the presence of the blocker of Smo activation SANT-1 (Chen et al., 2002) [$n \geq 3$ for each treatment; Fig. 4(D,E)], confirming that its expression requires Shh signaling at these later stages of development as well.

To examine whether the FGF and Shh pathways could act in concert to activate *Ptch2* expression, we cultured neural tube explants without the floor plate [and therefore without a source of Shh; Fig. 4(F)] in the presence of FGF4 and Shh separately or in combination. After 4 h exposure to FGF4, *Ptch2* expression was only slightly increased with respect to

control BSA treated explants [*n* = 7 for each treatment; Fig. 4(G,H)], whereas Shh activated *Ptch2* expression to moderate levels [*n* = 7; Fig. 4(I)]. By contrast, the levels of *Ptch2* expression were dramatically increased in the presence of both Shh and FGF, suggesting a synergistic effect [*n* = 8; Fig. 4(J)].

The limited increase in *Ptch2* expression with the FGF4 treatment in the absence of a Shh source suggested that FGF requires Shh signaling to promote efficiently *Ptch2* transcription. As expected, *Ptch2* mRNA levels in pNT explants that included the floor plate [Fig. 4(K)] were decreased upon 4 h exposure to the Smo blocker SANT-1 [*n* = 8 for each treatment; Fig. 4(L,M)] and its induction by FGF was blocked in the presence of the SANT-1 inhibitor [*n* = 8, Fig. 4(N,O)]. In summary, these results indicate that the strong caudal expression of *Ptch2* requires the concerted action of both Shh and FGF signaling.

The *Ptch2* Genomic Region Contains a Regulatory Element Responsive to Gli and Etv4 Factors Combination

A number of MAPK dependent FGF signaling events are mediated by transcription factors of the ETS family such as Etv3, Etv4 and Etv5 (Raible and Brand, 2001; Roehl and Nusslein-Volhard, 2001; Brent and Tabin, 2004). To examine whether FGF action on Shh signaling could be mediated through these effectors, we electroporated either *Fgf8b-pCIG* or *Etv4-pCIG* and examined the expression of ventral genes. Both constructs caused a severe down-regulation of Nkx2.2, Olig2, and Nkx6.1 expression in the ventral neural tube 20 h postelectroporation [*Fgf8*: *n* = 5/6, 7/7, and 7/7, respectively; *Etv4*: *n* = 6/6, 7/7, and 7/7, respectively; Fig. 5(A-D)] whereas no changes were observed in control electroporated embryos [Fig. 1(A,B)]. In some *Etv4-pCIG* electroporated embryos, we also observed disorganization of dorsal cells accompanied with ectopic intermediate and dorsal activation of Olig2 and Nkx2 (*n* = 4/6; Supporting Information Fig. 5) but this may reflect the interaction of Etv4 with dorsal specific pathways and is not explored here.

These results, indicating that Etv4 may be one of the effectors of the FGF signal in the neural tube and the rapid activation of *Ptch2* by the Shh and FGF pathways, suggest that *Ptch2* transcription may be directly regulated by the combined activity of Gli and ETS factors. We thus searched the chick *Ptch2* locus for the presence of conserved cis-regulatory sites that could respond to these transcription factors. *Ptch2* regulatory regions controlled by Gli activity have been described in mouse (Vokes et al., 2007; Holtz et al., 2013) and in zebrafish (Wang et al., 2013). Comparison of the chick *Ptch2* locus with that of other vertebrates revealed a conserved region (CR) with a putative Gli binding site (GBS) and a consensus ETS binding site [Fig. 5(E)] located in intron 2 [CR-intron2; present in fish (Wang et al., 2013), bird and reptile *Ptch2* genes; Supporting Information Fig. 6(A)].

To determine whether this region may mediate the activation of *Ptch2* transcription in response to combined FGF and Shh exposure, we examined its activity using a luciferase reporter vector where we inserted a 787 bp fragment containing CR-Intron 2, [Fig. 5(F)]. Embryos electroporated with a *Gli* activator (*GliA*) or with *Etv4* did not change luciferase levels significantly (ANOVA followed by Tamhane posthoc test) with respect to control *PCIG* [Fig. 5(F)]. Interestingly, combined electroporation of *GliA* and *Etv4* did increase the

levels of luciferase activity driven by this fragment up to (4.8±0.8) fold with respect to control PCIG [Fig. 5(F)].

These results suggest that the genomic fragment located in the second intron of *Ptch2* contains a cis-regulatory module that drives *Ptch2* expression in response to combined Shh-Gli and FGF/Etv4 signaling. This region may therefore be responsible for the expression of *Ptch2* in the transition zone region where both Shh and FGF signals coincide.

FGF Signaling is Required for *Ptch2* Expression and Ventral Patterning in Mouse Embryos

Caudal FGF signaling is also active in mammalian embryos suggesting that the regulation of *Ptch2* expression by FGF signaling could be conserved among vertebrates. Previous reports have described only low levels of mouse *Ptch2* mRNA expression in the developing ventral spinal cord (Motoyama et al., 1998) but with an improved *Ptch2 in situ* hybridization probe (see Methods), we observed strong gene expression in the ventral neural tube, especially at the level of the caudal neural tube at embryonic stages E9.5-E10.5 [Fig. 6(A,B)].

To address the possibility that FGF signaling could control *Ptch2* expression in mouse embryos, we deleted *Fgfr1* specifically in the caudal neural tissue and underlying mesoderm using a transgenic TCre line (Perantoni et al., 2005; Wahl et al., 2007). Stage E9.5-10 *TCre; Fgfr1*$^{flox/null}$ mutant embryos showed no or very low levels of *Ptch2* expression in the caudal neural tube [n = 4/6; Fig. 6(D,D′)] in comparison with their control *TCre; Fgfr1*$^{flox/+}$ siblings [n = 7; Fig. 6(C,C′)], indicating that FGF signaling is required for *Ptch2* expression during mouse neural development.

At caudal levels of E10-10.5 mutant embryos, we observed a neuroepitelial diverticulum as a ventral invagination of the neural tube or even a separate tube between the neural tube and the notochord [n = 12/13; Fig. 6(F,G)], which was never observed in their control siblings [n = 0/7; Fig. 6(E)]. This diverticulum formed by ventral neural progenitors expressing Nkx6.1 [Fig. 6(F′,G′)] is reminiscent of the ectopic neural tube described for a conditional double *Fgf4/Fgf8* mutant (Boulet and Capecchi, 2012) and may be related to changes in cell proliferation and morphogenesis or in mesoderm *versus* neural cell fate assignment and has not been further explored here.

To identify possible differences in ventral specification in mutant embryos with respect to controls, we analysed expression of Nkx6.1 and Olig2 focusing in the caudal spinal cord. Changes in ventral progenitor domains are difficult to assess in caudal regions as the borders of the domains are still dynamic and depend on the precise rostro-caudal level. However, the analysis of Nkx6.1 expression at a rostro-caudal level corresponding to onset of Olig2 expression (where only 2–11 Olig2$^+$ cells are present) showed an enlarged Nkx6.1 domain in mutants [69.2±11.2 Nkx6.1$^+$ cells; n = 9; Fig. 6(F′,G′H)] in comparison with controls [21.8±6.9 Nkx6.1$^+$ cells; n = 5; Fig. 6(E′,H)]. These changes in the number of Nkx6.1$^+$ neural progenitors are compatible with a broader initial activation of Shh signaling in the caudal neural tube owing to the reduced *Ptch2* expression in the caudal neural tube of mutant embryos.

Furthermore, to examine whether precocious activation of Shh signaling occurred in the mutants, we measured the distance that separates the rostro-caudal level where the ventral markers Olig2 and Nkx6.1 first appear and the level at which the notochord displays its characteristic rod shape (see methods for measurement details). Olig2 expression started at the level of the rod-shaped notochord in both mutant ($n = 6$) and control embryos ($n = 6$). By contrast, Nkx6.1 expression started around 200±25 μm caudal to the beginning of the rod-shaped notochord in mutant embryos whereas this distance was only about 60±27 μm in controls. As a result, the distance that separates the onset of Nkx6.1 and Olig2 was 60±12 μm in control embryos ($n = 5$) and increased to 155±23 μm in mutants [$n = 12$; Fig. 6(I)]. These data suggest that the ventral marker Nkx6.1 is expressed precociously in *Fgfr1* mutants.

Overall, these data support the conclusion that there is an evolutionary conservation in the control of the onset of ventral gene expression in the neural tube, governed by caudal FGF signaling regulation of *Ptch2* expression.

DISCUSSION

FGF Signaling Promotes a Negative Feedback Loop of the Shh Pathway at the Onset of Ventral Patterning

Ventral patterning is sustained by a complex gene regulatory network governed by Shh signaling and modulated by other signaling pathways. Here we have reported the novel observation that the FGF signaling pathway, acting at the initial stages of Shh signaling, is required for the proper restriction of ventral progenitor identity. We have also shown that FGF enhances the ability of Shh to promote the expression of *Ptch2*, a receptor and negative regulator of the Shh pathway (Briscoe et al., 2001; Holtz et al., 2013) and may thus attenuate the response to Shh and delay the onset of ventral patterning (summary in Fig. 7).

The mechanism of Shh signaling regulation by FGF described here reveals a specific feature of the Shh receptor gene *Ptch2* which is considered as a modulator of the Shh pathway activity [(Holtz et al., 2013; Alfaro et al., 2014) and our results]. Similarly to Ptch1, Ptch2 interacts with Shh and Smo (Carpenter et al., 1998) and blocks, albeit less efficiently than Ptch1, the activation of a Gli reporter *in vitro* (Rahnama et al., 2004; Nieuwenhuis et al., 2006; Holtz et al., 2013). Whereas mutations in mouse *Ptch1* result in a dramatic upregulation of Shh pathway activity (Goodrich et al., 1997), the requirement of *Ptch2* in mouse has so far been revealed when the levels of *Ptch1* are compromised (Lee et al., 2006; Nieuwenhuis et al., 2006; Holtz et al., 2013; Zhulyn et al., 2015) suggesting that its role may be at play within a particular time window or when developmental conditions are suboptimal.

As FGF8 production is tightly linked to the elongation process, it may serve as a sensor of caudal elongation and we propose that the FGF-*Ptch2* network may precisely coordinate the onset of ventral patterning to axis extension. Our results, thus, place *Ptch2* at the centre of the coordination of axial extension and ventral patterning initiation. They also suggest a role of *Ptch2* in conferring robustness in patterning under fluctuations in the elongation process.

FGF Signaling Modulates Several Signaling Pathways during Dorsoventral Patterning

Here we have focused on the role of FGF as a factor that limits Shh signaling activity. However, our results showing stronger ventral patterning defects associated to *FGF8* or *Etv4* overexpression in comparison with *Ptch2* overexpression indicate that Ptch2 is not the sole mediator of the effect of FGF signaling on ventral specification. Indeed, FGF also affects the onset of other signaling pathways involved in spinal cord patterning such as BMP and Wnt dorsally and retinoic acid (RA) throughout the DV axis (Diez del Corral et al., 2003; Novitch et al., 2003; Olivera-Martinez and Storey, 2007; Martinez-Morales et al., 2011; Sasai et al., 2014).

RA signaling is active at the level of the somites and is required for the expression of a subset of ventral specification genes (Diez del Corral et al., 2003; Olivera-Martinez and Storey, 2007). As FGF restrains RA signaling in the neural tube, the alterations due to changes in FGF could be indirectly attributed to changes in RA. However, that is not the case as not all genes affected by FGF are dependent on RA (Diez del Corral et al., 2003; Novitch et al., 2003) and furthermore, RA signaling is not changed caudally in the conditional *Fgfr* mutant used in our work (Wahl et al., 2007).

FGF can also downregulate expression of intermediate genes normally repressed by Shh such as *Pax6* and *Irx3* (Bertrand et al., 2000; Diez del Corral et al., 2003; Novitch et al., 2003) through a mechanism that involves chromatin compaction and changes in nuclear position of the *Pax6* and *Irx3* loci (Patel et al., 2013). As these intermediate patterning genes inhibit Olig2 and Nkx2.2, respectively (Briscoe et al., 2000; Novitch et al., 2001), the manipulation of FGF levels may also affect Olig2 and Nkx2.2 indirectly through an effect on intermediate genes. This may explain some discrepancies between our FGF results and previous data showing that *FGF8* overexpression in chicken does not reduce Olig2 and Nkx2.2 levels (Novitch et al., 2003). We propose that the results of misexpression experiments may differ depending on temporal and space windows used for *FGF8* overexpression, earlier and more caudal in our case. Our loss-of-function experiments reveal that FGF is required for the dorso-ventral restriction of Olig2 or Nkx2.2 domains but these domains would be further refined by the repression activities of Irx3 and Pax6 (Briscoe et al., 2000; Novitch et al., 2001).

In addition, transient exposure to FGF signaling has been recently shown to be important for floor plate specification (Sasai et al., 2014) and thus the overall picture that emerges from these results is that of a highly interconnected gene regulatory network that sustains dorso-ventral patterning, with FGF signaling acting as a crucial modulator of the initiation of Shh dependent ventral patterning as well as of intermediate and dorsal patterning including neural crest specification.

FGF Signaling as a Modulator of the Shh Pathway in Multiple Contexts

Although we have identified a previously unreported molecular mechanism for FGF-mediated interference with the Shh pathway in the spinal cord, other interactions between these two pathways have been described in other contexts during development (Riobo et al., 2006). In most of the described cases, however, they display cooperative and not

antagonistic functions (Ye et al., 1998; Storm et al., 2006; Blaess et al., 2008). In a few cases, the regulation of Shh components by FGF has been identified and for example FGF can activate Gli2 expression in early *Xenopus* mesoderm patterning (Brewster et al., 2000). One interesting situation is found during limb development where both cooperative and antagonistic relations have been described. In this case, FGF is required for initiation and maintenance of Shh expression but it also downregulates *Shh* transcription through a limb specific enhancer (Lettice et al., 2003; Mao et al., 2009; Zhang et al., 2009; Lettice et al., 2012).

FGF and Shh are also implicated in the control of proliferation during development and in cancer. Antagonism of the two pathways has been suggested in pathological situations such as medulloblastoma cells produced in *Ptch1*$^{+/-}$ mutant mice in which bFGF acts as a potent inhibitor of proliferation (Fogarty et al., 2007; Emmenegger et al., 2012). Considering that a reduction of *Ptch2* can exacerbate the formation of medulloblastomas (Lee et al., 2006), it is tempting to propose that one possible mechanism for the anti-proliferative activity of FGF in this context could be an increase in *Ptch2* levels.

Finally, a mechanism of negative feedback loop control, as the one we describe here to tune the onset of a critical signaling such as the Shh pathway, may be a common strategy used in other gene regulatory networks in development or in tissue homeostasis to provide robustness at the initial stages of signaling.

Supplementary Material

Refer to Web version on PubMed Central for supplementary material.

Acknowledgments

The authors are grateful to K. Storey for comments on the manuscript and to J.M. Frade for support during the initial stages of the project. The authors thank E. Martí, S. Martinez, T. Oosterveen, L. Puelles, L. Sánchez-Arrones, T Schimmang, C. Tabin, and C. Weijer for DNA templates and for expression constructs. The authors are grateful to C. Bahamon, M. Ciorraga, M.C. Escudero, C. Oueslati, and O. Parreño for technical assistance. The authors thank J. Briscoe and N. Sasai for sharing results prior to publication.

Contract grant sponsor: Spanish government; contract grant numbers: BFU2014-57494-R, BFU2011-29490, BFU2010-15665, BFU2005-02972 (to A. M. and R. D.) and BFU2007-61774, BFU2010-16031-P (to P. B.).

Contract grant sponsor: Madrid Local Government; contract grant number: CCG07-CSIC/SAL-1930 (to R. D.).

Contract grant sponsor: CIBERER (to P.B.).

REFERENCES

Alfaro AC, Roberts B, Kwong L, Bijlsma MF, Roelink H. 2014 Ptch2 mediates the Shh response in Ptch1−/− cells. Development 141:3331–3339. [PubMed: 25085974]

Bertrand N, Medevielle F, Pituello F. 2000 FGF signaling controls the timing of Pax6 activation in the neural tube. Development 127:4837–4843. [PubMed: 11044398]

Blaess S, Stephen D, Joyner AL. 2008 Gli3 coordinates three-dimensional patterning and growth of the tectum and cerebellum by integrating Shh and Fgf8 signaling. Development 135:2093–2103. [PubMed: 18480159]

Boulet AM, Capecchi MR. 2012 Signaling by FGF4 and FGF8 is required for axial elongation of the mouse embryo. Dev Biol 371:235–245. [PubMed: 22954964]

Brent AE, Tabin CJ. 2004 FGF acts directly on the somitic tendon progenitors through the Ets transcription factors Pea3 and Erm to regulate scleraxis expression. Development 131:3885–3896. [PubMed: 15253939]

Brewster R, Mullor JL, Ruiz i Altaba A. 2000 Gli2 functions in FGF signaling during antero-posterior patterning. Development 127:4395–4405. [PubMed: 11003839]

Briscoe J, Chen Y, Jessell TM, Struhl G. 2001 A hedgehog-insensitive form of patched provides evidence for direct long-range morphogen activity of sonic hedgehog in the neural tube. Mol Cell 7:1279–1291. [PubMed: 11430830]

Briscoe J, Pierani A, Jessell TM, Ericson J. 2000 A homeo-domain protein code specifies progenitor cell identity and neuronal fate in the ventral neural tube. Cell 101:435–445. [PubMed: 10830170]

Brown JM, Storey KG. 2000 A region of the vertebrate neural plate in which neighbouring cells can adopt neural or epidermal cell fates. Curr Biol 10:869–872. [PubMed: 10899008]

Cai J, Xu X, Yin H, Wu R, Modderman G, Chen Y, Jensen J, et al. 2000 Evidence for the differential regulation of Nkx-6.1 expression in the ventral spinal cord and foregut by Shh-dependent and -independent mechanisms. Genesis 27:6–11. [PubMed: 10862150]

Carpenter D, Stone DM, Brush J, Ryan A, Armanini M, Frantz G, Rosenthal A, et al. 1998 Characterization of two patched receptors for the vertebrate hedgehog protein family. Proc Natl Acad Sci USA 95:13630–13634. [PubMed: 9811851]

Carre W, Wang X, Porter TE, Nys Y, Tang J, Bernberg E, Morgan R, et al. 2006 Chicken genomics resource: sequencing and annotation of 35,407 ESTs from single and multiple tissue cDNA libraries and CAP3 assembly of a chicken gene index. Physiol Genomics 25:514–524. [PubMed: 16554550]

Chen JK, Taipale J, Young KE, Maiti T, Beachy PA. 2002 Small molecule modulation of Smoothened activity. Proc Natl Acad Sci USA 99:14071–14076. [PubMed: 12391318]

Dessaud E, McMahon AP, Briscoe J. 2008 Pattern formation in the vertebrate neural tube: a sonic hedgehog morphogen-regulated transcriptional network. Development 135:2489–2503. [PubMed: 18621990]

Diez del Corral R, Breitkreuz DN, Storey KG. 2002 Onset of neuronal differentiation is regulated by paraxial mesoderm and requires attenuation of FGF signaling. Development 129:1681–1691. [PubMed: 11923204]

Diez del Corral R, Olivera-Martinez I, Goriely A, Gale E, Maden M, Storey KG. 2003 Opposing FGF and retinoid pathways control ventral neural pattern, neuronal differentiation, and segmentation during body axis extension. Neuron 40:65–79. [PubMed: 14527434]

Dominguez-Frutos E, Vendrell V, Alvarez Y, Zelarayan LC, Lopez-Hernandez I, Ros M, Schimmang T. 2009 Tissue-specific requirements for FGF8 during early inner ear development. Mech Dev 126:873–881. [PubMed: 19619645]

Emmenegger BA, Hwang EI, Moore C, Markant SL, Brun SN, Dutton JW, Read TA, et al. 2012 Distinct roles for fibroblast growth factor signaling in cerebellar development and medulloblastoma. Oncogene 32:4181–4188. [PubMed: 23045271]

Fogarty MP, Emmenegger BA, Grasfeder LL, Oliver TG, Wechsler-Reya RJ. 2007 Fibroblast growth factor blocks Sonic hedgehog signaling in neuronal precursors and tumor cells. Proc Natl Acad Sci USA 104:2973–2978. [PubMed: 17299056]

Goodrich LV, Johnson RL, Milenkovic L, McMahon JA, Scott MP. 1996 Conservation of the hedgehog/patched signaling pathway from flies to mice: induction of a mouse patched gene by Hedgehog. Genes Dev 10:301–312. [PubMed: 8595881]

Goodrich LV, Milenkovic L, Higgins KM, Scott MP. 1997 Altered neural cell fates and medulloblastoma in mouse patched mutants. Science 277:1109–1113. [PubMed: 9262482]

Hallikas O, Palin K, Sinjushina N, Rautiainen R, Partanen J, Ukkonen E, Taipale J. 2006 Genome-wide prediction of mammalian enhancers based on analysis of transcription-factor binding affinity. Cell 124:47–59. [PubMed: 16413481]

Holtz AM, Peterson KA, Nishi Y, Morin S, Song JY, Charron F, McMahon AP, et al. 2013 Essential role for ligand-dependent feedback antagonism of vertebrate hedgehog signaling by PTCH1, PTCH2 and HHIP1 during neural patterning. Development 140:3423–3434. [PubMed: 23900540]

Jeong J, McMahon AP. 2005 Growth and pattern of the mammalian neural tube are governed by partially overlapping feedback activities of the hedgehog antagonists patched 1 and Hhip1. Development 132:143–154. [PubMed: 15576403]

Jessell TM. 2000 Neuronal specification in the spinal cord: inductive signals and transcriptional codes. Nat Rev Genet 1:20–29. [PubMed: 11262869]

Kinzler KW, Vogelstein B. 1990 The GLI gene encodes a nuclear protein which binds specific sequences in the human genome. Mol Cell Biol 10:634–642. [PubMed: 2105456]

Lee J, Platt KA, Censullo P, Ruiz i Altaba A. 1997 Gli1 is a target of Sonic hedgehog that induces ventral neural tube development. Development 124:2537–2552. [PubMed: 9216996]

Lee Y, Miller HL, Russell HR, Boyd K, Curran T, McKinnon PJ. 2006 Patched2 modulates tumorigenesis in patched1 heterozygous mice. Cancer Res 66:6964–6971. [PubMed: 16849540]

Lettice LA, Heaney SJ, Purdie LA, Li L, de Beer P, Oostra BA, Goode D, et al. 2003 A long-range Shh enhancer regulates expression in the developing limb and fin and is associated with preaxial polydactyly. Hum Mol Genet 12:1725–1735. [PubMed: 12837695]

Lettice LA, Williamson I, Wiltshire JH, Peluso S, Devenney PS, Hill AE, Essafi A, et al. 2012 Opposing functions of the ETS factor family define Shh spatial expression in limb buds and underlie polydactyly. Dev Cell 22:459–467. [PubMed: 22340503]

Lu QR, Yuk D, Alberta JA, Zhu Z, Pawlitzky I, Chan J, McMahon AP, et al. 2000 Sonic hedgehog–regulated oligodendrocyte lineage genes encoding bHLH proteins in the mammalian central nervous system. Neuron 25:317–329. [PubMed: 10719888]

Mao J, McGlinn E, Huang P, Tabin CJ, McMahon AP. 2009 Fgf-dependent Etv4/5 activity is required for posterior restriction of Sonic Hedgehog and promoting outgrowth of the vertebrate limb. Dev Cell 16:600–606. [PubMed: 19386268]

Marigo V, Tabin CJ. 1996 Regulation of patched by sonic hedgehog in the developing neural tube. Proc Natl Acad Sci USA 93:9346–9351. [PubMed: 8790332]

Martinez-Morales PL, Diez Del Corral R, Olivera-Martinez I, Quiroga AC, Das RM, Barbas JA, Storey KG, et al. 2011 FGF and retinoic acid activity gradients control the timing of neural crest cell emigration in the trunk. J Cell Biol 194:489–503. [PubMed: 21807879]

Mathis L, Kulesa PM, Fraser SE. 2001 FGF receptor signaling is required to maintain neural progenitors during Hensen's node progression. Nat Cell Biol 3:559–566. [PubMed: 11389440]

Megason SG, McMahon AP. 2002 A mitogen gradient of dorsal midline Wnts organizes growth in the CNS. Development 129:2087–2098. [PubMed: 11959819]

Minowada G, Jarvis LA, Chi CL, Neubuser A, Sun X, Hacohen N, Krasnow MA, et al. 1999 Vertebrate Sprouty genes are induced by FGF signaling and can cause chondrodysplasia when overexpressed. Development 126:4465–4475. [PubMed: 10498682]

Mohammadi M, Froum S, Hamby JM, Schroeder MC, Panek RL, Lu GH, Eliseenkova AV, et al. 1998 Crystal structure of an angiogenesis inhibitor bound to the FGF receptor tyrosine kinase domain. EMBO J 17:5896–5904. [PubMed: 9774334]

Motoyama J, Heng H, Crackower MA, Takabatake T, Takeshima K, Tsui LC, Hui C. 1998 Overlapping and non-overlapping Ptch2 expression with Shh during mouse embryogenesis. Mech Dev 78:81–84. [PubMed: 9858693]

Nieuwenhuis E, Motoyama J, Barnfield PC, Yoshikawa Y, Zhang X, Mo R, Crackower MA, et al. 2006 Mice with a targeted mutation of patched2 are viable but develop alopecia and epidermal hyperplasia. Mol Cell Biol 26:6609–6622. [PubMed: 16914743]

Novitch BG, Chen AI, Jessell TM. 2001 Coordinate regulation of motor neuron subtype identity and pan-neuronal properties by the bHLH repressor Olig2. Neuron 31:773–789. [PubMed: 11567616]

Novitch BG, Wichterle H, Jessell TM, Sockanathan S. 2003 A requirement for retinoic acid-mediated transcriptional activation in ventral neural patterning and motor neuron specification. Neuron 40:81–95. [PubMed: 14527435]

Olivera-Martinez I, Storey KG. 2007 Wnt signals provide a timing mechanism for the FGF-retinoid differentiation switch during vertebrate body axis extension. Development 134:2125–2135. [PubMed: 17507413]

Park HL, Bai C, Platt KA, Matise MP, Beeghly A, Hui CC, Nakashima M, et al. 2000 Mouse Gli1 mutants are viable but have defects in SHH signaling in combination with a Gli2 mutation. Development 127:1593–1605. [PubMed: 10725236]

Patel NS, Rhinn M, Semprich CI, Halley PA, Dolle P, Bickmore WA, Storey KG. 2013 FGF signaling regulates chromatin organisation during neural differentiation via mechanisms that can be uncoupled from transcription. PLoS Genet 9:e1003614 [PubMed: 23874217]

Pearse RV II, Vogan KJ, Tabin CJ. 2001 Ptc1 and Ptc2 transcripts provide distinct readouts of Hedgehog signaling activity during chick embryogenesis. Dev Biol 239:15–29. [PubMed: 11784016]

Perantoni AO, Timofeeva O, Naillat F, Richman C, Pajni-Underwood S, Wilson C, Vainio S, et al. 2005 Inactivation of FGF8 in early mesoderm reveals an essential role in kidney development. Development 132:3859–3871. [PubMed: 16049111]

Quirk J, van den Heuvel M, Henrique D, Marigo V, Jones TA, Tabin C, Ingham PW. 1997 The smoothened gene and hedgehog signal transduction in Drosophila and vertebrate development. Cold Spring Harb Symp Quant Biol 62:217–226. [PubMed: 9598354]

Rahnama F, Toftgard R, Zaphiropoulos PG. 2004 Distinct roles of PTCH2 splice variants in Hedgehog signaling. Biochem J 378:325–334. [PubMed: 14613484]

Raible F, Brand M. 2001 Tight transcriptional control of the ETS domain factors Erm and Pea3 by Fgf signaling during early zebrafish development. Mech Dev 107:105–117. [PubMed: 11520667]

Ribes V, Balaskas N, Sasai N, Cruz C, Dessaud E, Cayuso J, Tozer S, et al. 2010 Distinct Sonic Hedgehog signaling dynamics specify floor plate and ventral neuronal progenitors in the vertebrate neural tube. Genes Dev 24:1186–1200. [PubMed: 20516201]

Ribes V, Briscoe J. 2009 Establishing and interpreting graded Sonic Hedgehog signaling during vertebrate neural tube patterning: the role of negative feedback. Cold Spring Harb Perspect Biol 1:a002014 [PubMed: 20066087]

Riobo NA, Lu K, Emerson CP Jr. 2006 Hedgehog signal transduction: signal integration and cross talk in development and cancer. Cell Cycle 5:1612–1615. [PubMed: 16880744]

Roehl H, Nusslein-Volhard C. 2001 Zebrafish pea3 and erm are general targets of FGF8 signaling. Curr Biol 11:503–507. [PubMed: 11413000]

Sasai N, Kutejova E, Briscoe J. 2014 Integration of signals along orthogonal axes of the vertebrate neural tube controls progenitor competence and increases cell diversity. PLoS Biol 12:e1001907 [PubMed: 25026549]

Sebolt-Leopold JS, Dudley DT, Herrera R, Van Becelaere K, Wiland A, Gowan RC, Tecle H, et al. 1999 Blockade of the MAP kinase pathway suppresses growth of colon tumors in vivo. Nat Med 5:810–816. [PubMed: 10395327]

Stamataki D, Ulloa F, Tsoni SV, Mynett A, Briscoe J. 2005 A gradient of Gli activity mediates graded Sonic Hedgehog signaling in the neural tube. Genes Dev 19:626–641. [PubMed: 15741323]

Storm EE, Garel S, Borello U, Hebert JM, Martinez S, McConnell SK, Martin GR, et al. 2006 Dose-dependent functions of Fgf8 in regulating telencephalic patterning centers. Development 133:1831–1844. [PubMed: 16613831]

Takabatake T, Ogawa M, Takahashi TC, Mizuno M, Okamoto M, Takeshima K. 1997 Hedgehog and patched gene expression in adult ocular tissues. FEBS letters 410:485–489. [PubMed: 9237688]

Vokes SA, Ji H, McCuine S, Tenzen T, Giles S, Zhong S, Longabaugh WJ, Davidson EH, et al. 2007 Genomic characterization of Gli-activator targets in sonic hedgehog-mediated neural patterning. Development 134:1977–1989. [PubMed: 17442700]

Wahl MB, Deng C, Lewandoski M, Pourquie O. 2007 FGF signaling acts upstream of the NOTCH and WNT signaling pathways to control segmentation clock oscillations in mouse somitogenesis. Development 134:4033–4041. [PubMed: 17965051]

Wang X, Zhao Z, Muller J, Iyu A, Khng AJ, Guccione E, Ruan Y, et al. 2013 Targeted inactivation and identification of targets of the Gli2a transcription factor in the zebrafish. Biol Open 2:1203–1213. [PubMed: 24244857]

Wei GH, Badis G, Berger MF, Kivioja T, Palin K, Enge M, Bonke M, et al. 2010 Genome-wide analysis of ETS-family DNA-binding *in vitro* and *in vivo*. EMBO J 29:2147–2160. [PubMed: 20517297]

Xu X, Qiao W, Li C, Deng CX. 2002 Generation of Fgfr1 conditional knockout mice. Genesis 32:85–86. [PubMed: 11857785]

Yang X, Dormann D, Munsterberg AE, Weijer CJ. 2002 Cell movement patterns during gastrulation in the chick are controlled by positive and negative chemotaxis mediated by FGF4 and FGF8. Dev Cell 3:425–437. [PubMed: 12361604]

Ye W, shimamura K, Rubenstein JLR, Hynes MA, Rosenthal A. 1998 FGF and Shh signals control dopaminergic and serotonergic cell fate in the anterior neural ridge. Cell 93:755–766. [PubMed: 9630220]

Zhang Z, Verheyden JM, Hassell JA, Sun X. 2009 FGF-regulated Etv genes are essential for repressing Shh expression in mouse limb buds. Dev Cell 16:607–613. [PubMed: 19386269]

Zhulyn O, Nieuwenhuis E, Liu YC, Angers S, Hui CC. 2015 Ptch2 shares overlapping functions with Ptch1 in Smo regulation and limb development. Dev Biol 397:191–202. [PubMed: 25448692]

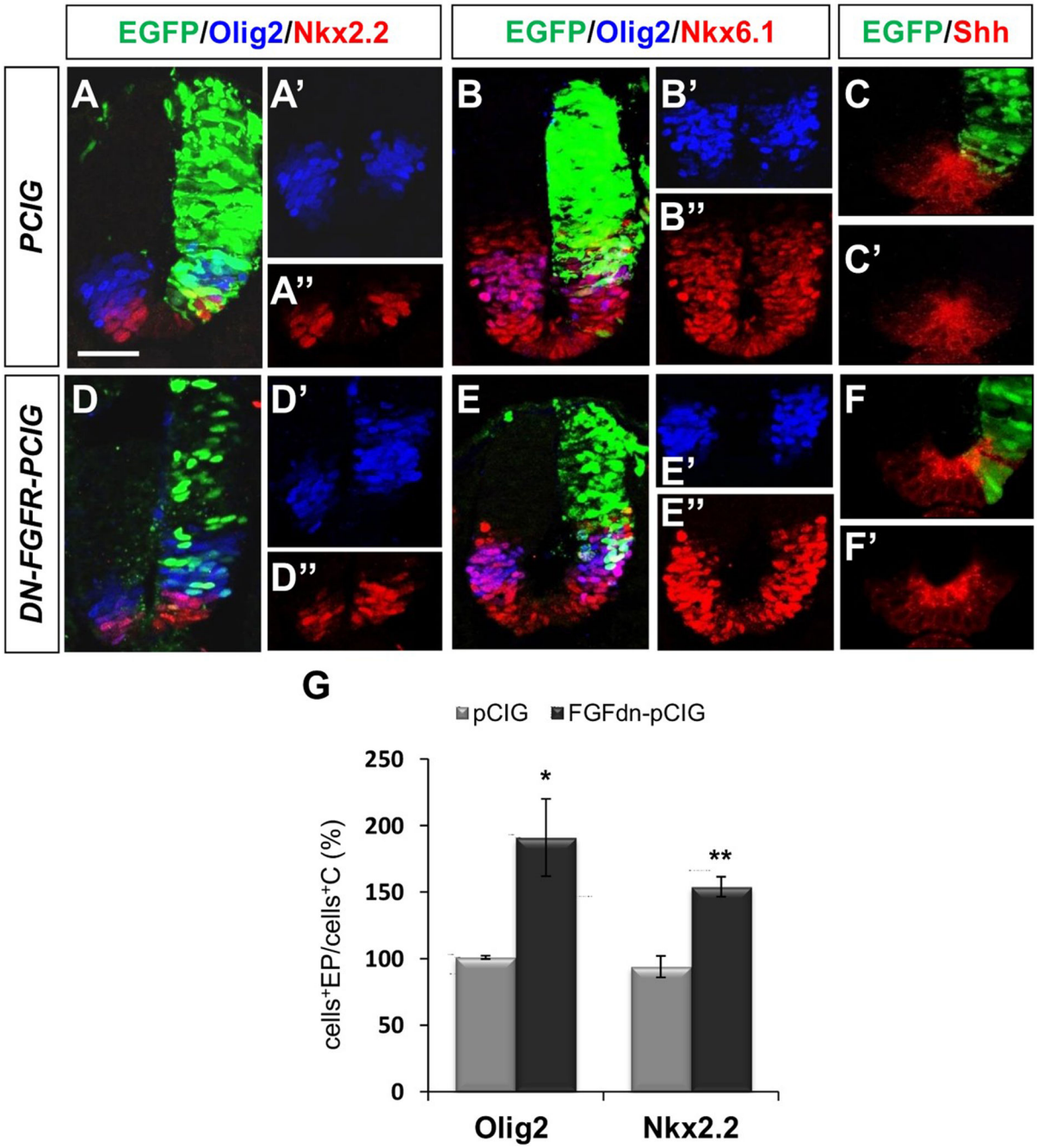

Figure 1.

FGF signaling is required for proper ventral patterning specification. (A–C) Control (*PCIG*) or (D–F) *DN-FGFR* electroporated neural tube sections showing the electroporated region in green (EGFP) and immunostaining for Olig2, Nkx2.2, Nkx6.1, and Shh as indicated. (A′–F′, A″–B″, D″–E″) Non-EGFP channel images. (G) Quantitation of the number of Olig2 and Nkx2.2 expressing cells in *PCIG* ($n = 6$ and 3, respectively) and *DN-FGFR* ($n = 5$ and 4, respectively) electroporated hemitubes with respect to corresponding control hemitubes.

Each bar represents mean±SEM (see methods). Scale bar: 30 μm. *$p < 0.05$ and ** $p < 0.01$ (Student's *t*-test).

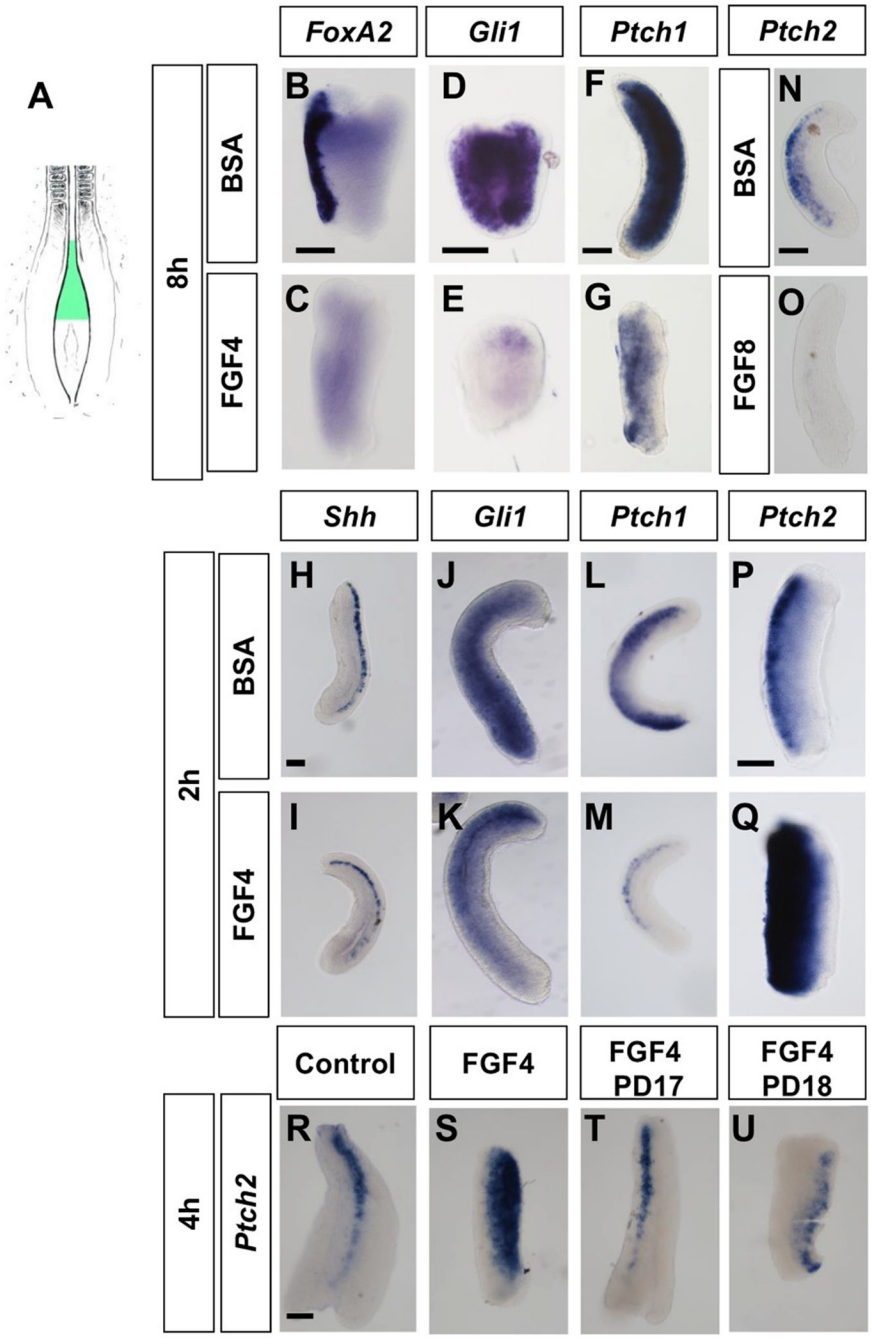

Figure 2.

FGF signaling upregulates *Ptch2* expression through the FGFR-MAPK pathway. (A) Diagram showing the ectoderm region used for the chick neural explant cultures shown in (B–U). (B–G) Expression of the Shh downstream targets *FoxA2, Gli1* and *Ptch1* in explants cultured for 8 h either in control conditions (B, D, F) or in the presence of FGF4 (C, E, G). (H–M) Expression of the Shh signaling components *Shh, Gli1, Ptch1* in explants cultured for 2 h either in control conditions or in the presence of FGF4 as indicated. (N, O) Expression of *Ptch2* in explants cultured for 8 h either in control conditions (N) or in the

presence of FGF8 (O). (P, Q) Expression of *Ptch2* in explants culture for 2 h either in control (P) or in the presence of FGF8 (Q). (R–U) Expression of *Ptch2* in explants cultured for 4 h in control conditions (R) or the presence of FGF4 (S), FGF4 and the FGFR antagonist PD173074 (T) or FGF4 and the MEK antagonist PD184352 (U). Scale bars: 100 μm (in B for B–C, in D for D-E., in F for F–G, in H for H–M, in N for N–O, in P for P–Q, and in R for R–U).

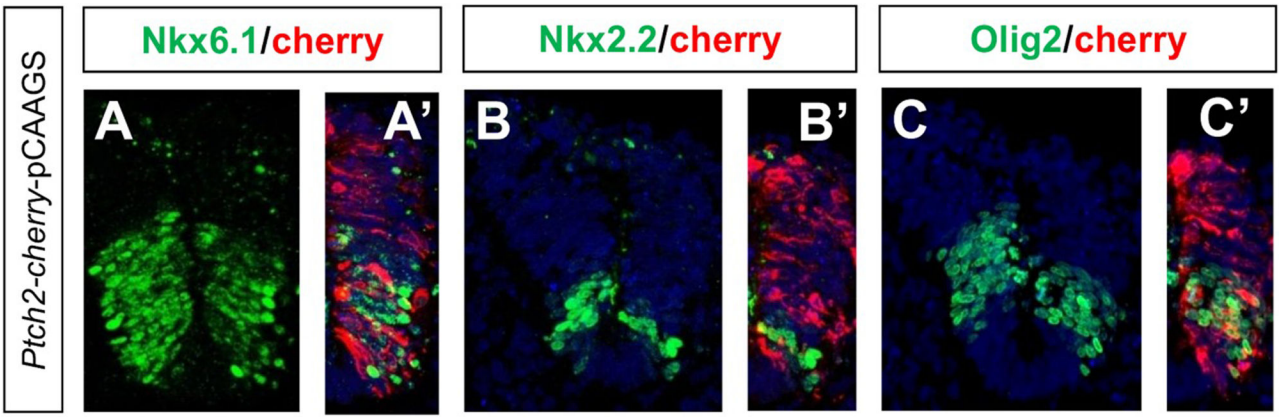

Figure 3.

Ptch2 overexpression reduces expression of ventral genes. (A–C) *mPtch2-Cherry* electroporated neural tube sections showing immunostaining for Nkx6.1, Nkx2.2, and Olig2 as indicated. (A'-C') Merge images showing the cherry channel.

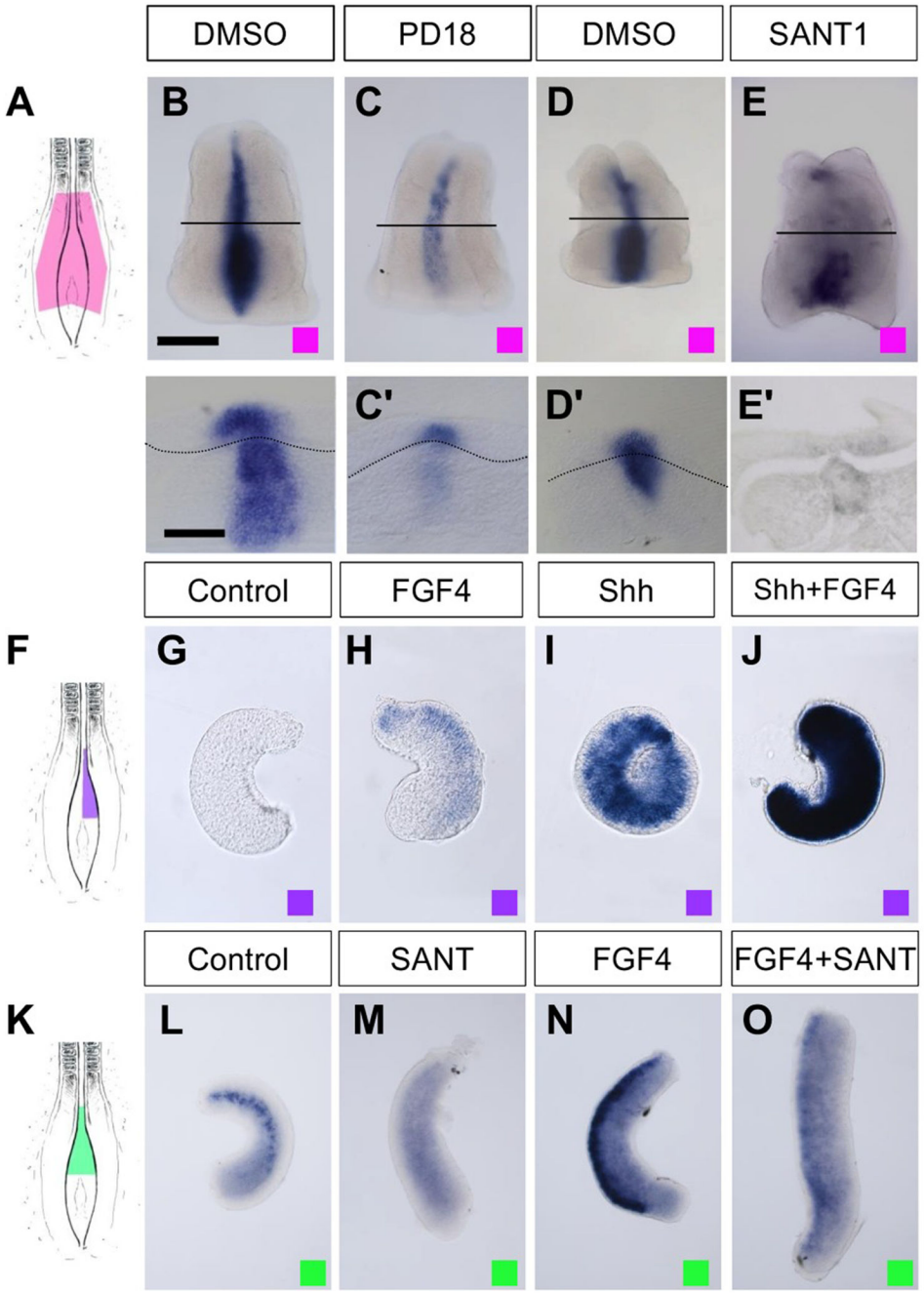

Figure 4.

FGF and Shh signaling control the onset of *Ptch2* expression. (A, F, K) Diagrams showing the regions used for explant cultures in the experiments shown in (B–E, G–J, L–O) as indicated with colour coded squares. Explants include either three germinal layers and node (A) or only ectoderm (F and K). (B–E) Expression of *Ptch2* in chick explants cultured for 4 h in control conditions (B, D) and in the presence of PD184352 (C) or SANT-1 (E). (B′–E′) are transverse sections. (G–J) Expression of *Ptch2* in chick neural explants devoid of floor plate cultured for 4 h in control conditions (G) or in the presence of the indicated factor (H–J). (L–O) Expression of *Ptch2* in chick neural explants cultured for 4 h in control conditions

(L) or in the presence of the indicated molecule (M–O). Scale bars: 200 μm in B (for B–E, G–J, and L–O) and 100 μm in B′ for (B′–E′).

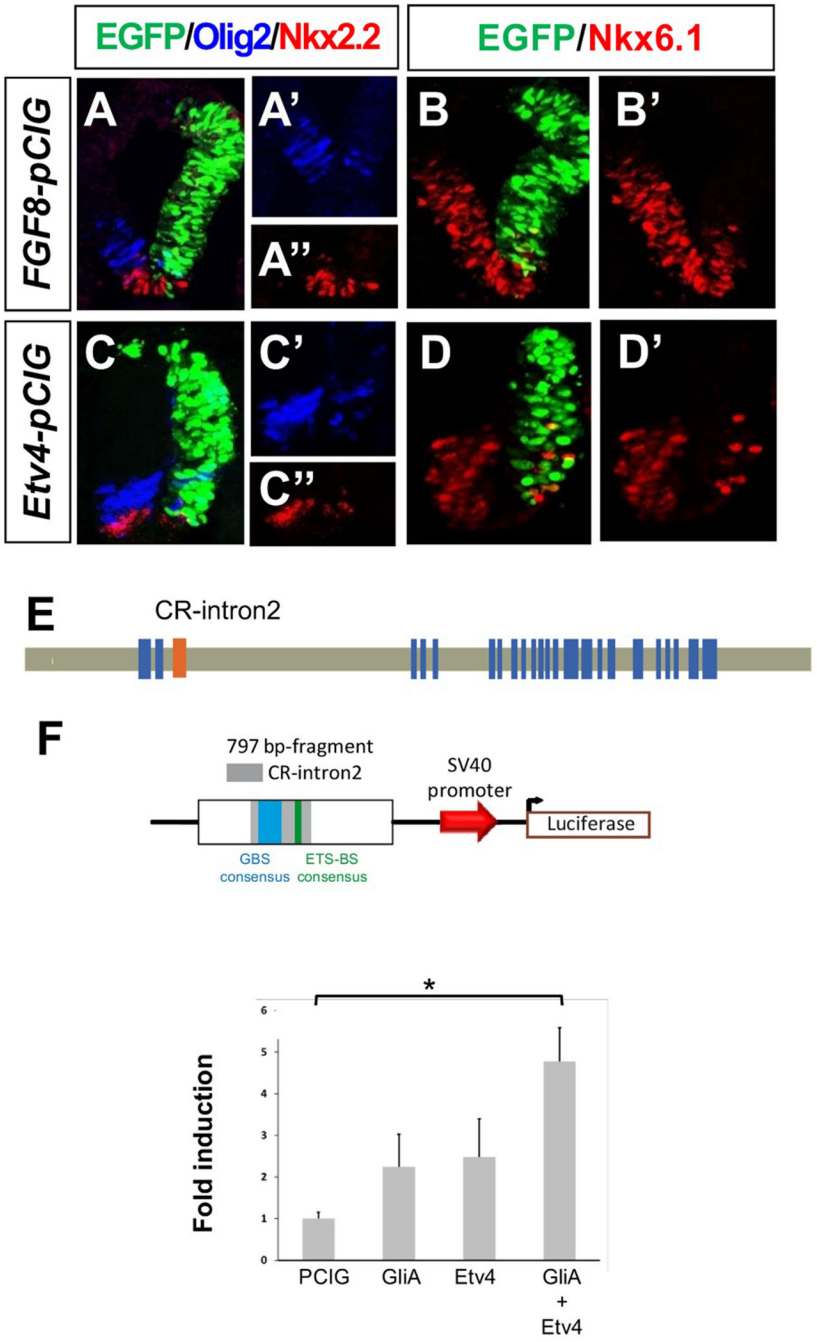

Figure 5.

The Etv4 transcription factor mimics the effect of FGF8 on ventral patterning genes and in combination with GliA can activate a regulatory region from the *Ptch2* locus. (A, B) *FGF8* or (C-D) *Etv4* electroporated neural tube sections showing the extent of electroporation in green (EGFP) and immunostaining for Olig2, Nkx2.2, Nkx6.1. (E) Diagram showing chick *Ptch2* genomic structure (blue rectangles indicate exons) and highlighting the localization of the conserved region in intron 2 (CR-intron2) that includes a Gli binding site consensus sequence. (F) Quantitative analysis of the transcriptional activity of the 797 bp-fragment-

luciferase plasmid (shown schematically above) following electroporation of *PCIG, GliA, Etv4*, or a combination of *GliA* and *Etv4* expression plasmids, as indicated. Each bar represents mean±SEM (see methods). *$p < 0.05$ (ANOVA followed by Tamhane *post hoc* test).

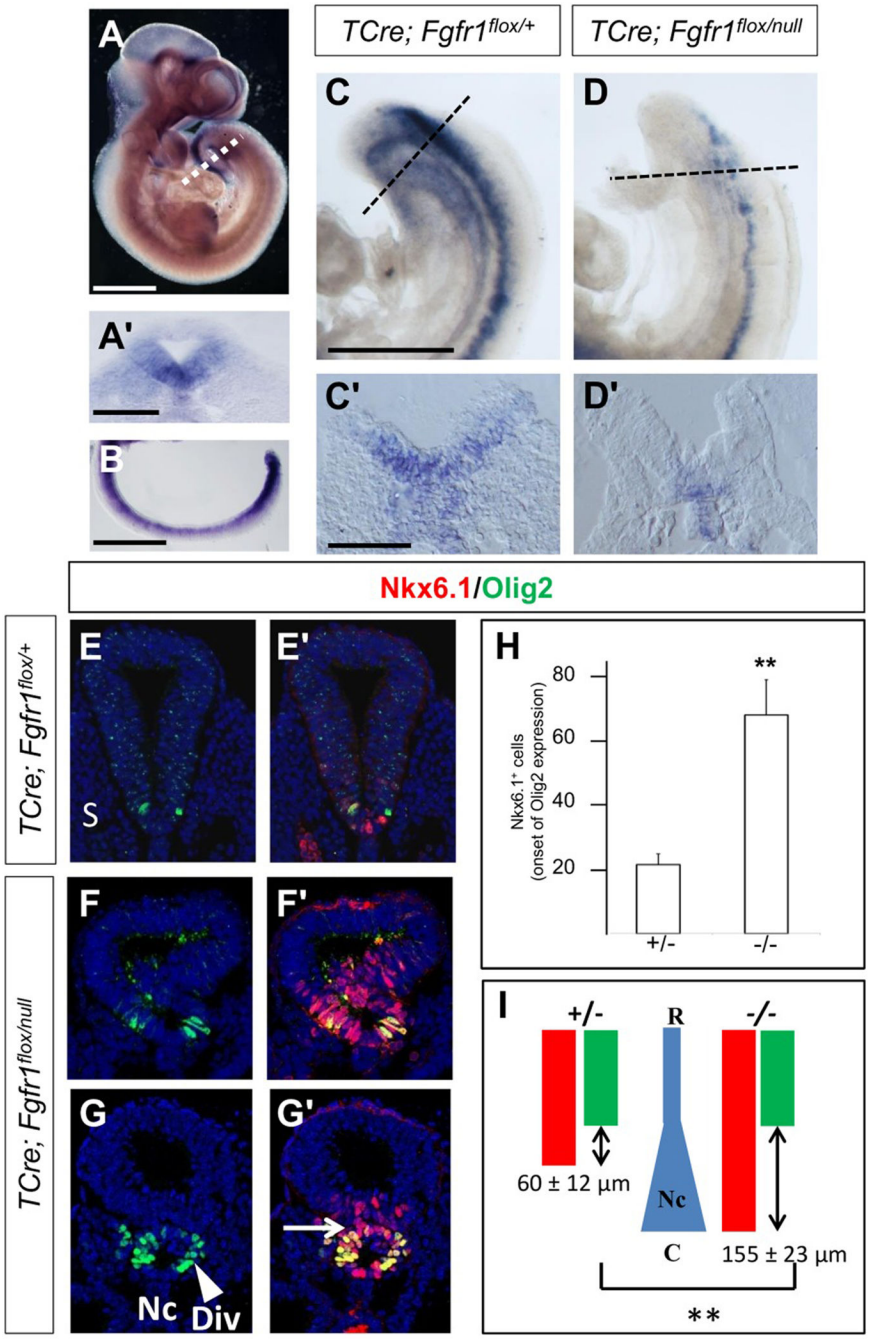

Figure 6.

FGF signaling is required for the onset of mouse *Ptch2* expression and for the initial ventral patterning of the neural tube in mouse embryos. (A, A′, B) Expression of *Ptch2* in stage E10.5 (A, A′) and E9.5 (B) mouse embryos in whole mount (A), in a transverse section (A′) at the level of the dotted line in (A) and in a dissected caudal neural tube (B). (C–C′, D–D′) Expression of *Ptch2* in E9.5 *TCre; Fgfr1*$^{flox/+}$ (C–C′) or in *TCre; Fgfr1*$^{flox/null}$ (D–D′) mouse embryos in whole mount (C, D) and in transverse sections (C′, D′). (E–E′, F–F′, G–G′) Transverse sections of E10.5 stage spinal cord of the indicated genotypes, showing the

expression of Olig2 and Nkx6.1 at caudal levels. (E–E′, F–F′) Sections corresponding to the region where the first Olig2 expressing cells appear in a *TCre; Fgfr1*$^{flox/+}$ embryo or in a *TCre; Fgfr1*$^{flox/null}$ embryo. (G–G′) Section showing the abnormal morphology of the neural tube of a *TCre; Fgfr1*$^{flox/null}$ embryo. (H) Quantification of the number of Nkx6.1^{+} cells at the spinal cord levels where the first Olig2 expressing cells appear in control and *TCre; Fgfr1*$^{flox/null}$ embryos. Each bar represents mean±SEM. (I) Diagram depicting the domains of Olig2 and Nkx6.1 along the rostral (R) to caudal (C) axis in *TCre; Fgfr1*$^{flox/+}$ and *TCre; Fgfr1*$^{flox/null}$ embryos. The rostrocaudal distance separating the initiation of Olig2 and Nkx6.1 expression is shown with a double arrowed symbol and mean±SEM are indicated. The changing shape of the notochord is also depicted in blue. Nc: Notochord, S: somite, Div: diverticulum, arrow points at the separation of the tube and the diverticulum, R: Rostral, C: Caudal. Scale bars: 500 μm (A), 100 μm (A′), 500 μm (B), 500 μm (C for C and D), 100 μm (C′ for C′ and D′). ** $p \leq 0{,}01$ (Student's t test).

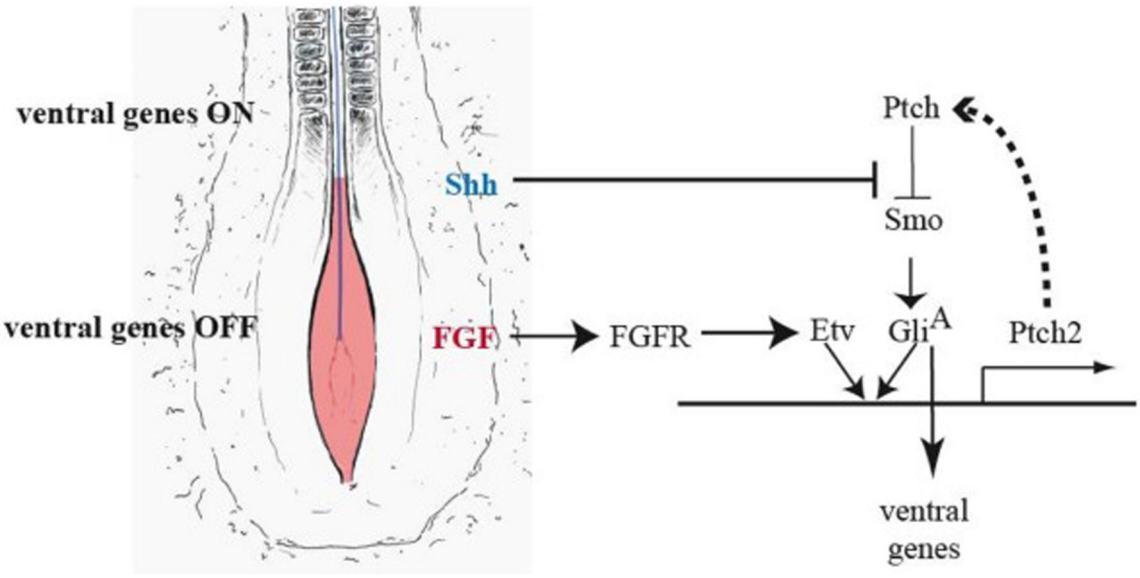

Figure 7.

Proposed model of FGF-mediated regulation of the Shh pathway in the spinal cord. Neural tube/plate cells adjacent to the presomitic mesoderm are exposed to FGF4/8 (red) and Shh (blue, produced by the underlying notochord). Shh triggers a gene regulatory network that activates downstream genes, including *Ptch2*, a component of a negative feedback loop of the pathway. In this region, FGF signaling further promotes *Ptch2* expression and therefore reinforces the negative feedback loop in the Shh pathway, delaying the onset of ventral gene expression.